Tellus
SERIES A
DYNAMIC
METEOROLOGY
AND OCEANOGRAPHY
PUBLISHED BY THE INTERNATIONAL METEOROLOGICAL INSTITUTE IN STOCKHOLM

Tellus (2008), 60A, 898–910

TELLUS

Spectral nudging in a spectral regional climate model

By RALUCA RADU[1]*, MICHEL DÉQUÉ[2] and SAMUEL SOMOT[2], [1]*National Meteorological Administration LNM, Bucharest, Romania;* [2]*Météo France CNRM/GMGEC CNRS/GAME, Toulouse, France*

(Manuscript received 11 October 2007; in final form 23 April 2008)

ABSTRACT

Spectral nudging, a dynamic downscaling method, has been used as a suitable approach to force a regional model to adopt prescribed large-scales over the entire domain, not just at the lateral boundaries, while developing realistic detailed regional features consistent with the large-scales. The aim of this study is to compare a global spectral climate model at high resolution (50 km) and a driven spectral regional climate model over Europe by using the so-called perfect model approach. The spectral nudging method is applied in order to achieve a better representation of large-scale climate over a limited domain. The results show that the regional model driven only at its lateral boundaries presents a summer warm bias in the middle of the domain. This bias disappears when spectral nudging is applied. On the other hand, the smallest scales which are not driven by the spectral nudging are not significantly affected by scale interaction. The only detrimental impact of spectral nudging is a slight precipitation increase in the upper quantiles of precipitation, which can be resolved by large-scale nudging of specific humidity.

1. Introduction

Nowadays, increasing interest in regional climate change and its impacts demand a high resolution description of the climate. However, running multicomponent global climate models (GCMs) at high resolutions remains computationally too expensive for long-term simulations. Even if a global climate model is able to resolve events taking place at the synoptic scales, the mesoscale events which are very important for the local climate cannot be resolved accurately with GCMs. Regional climate models (RCMs) can provide a more realistic representation of regional scale features, which current GCMs do not resolve, at an affordable computational cost. In fact, RCMs can add higher resolution details to GCMs simulations and also produce large-scale characteristics in agreement with the GCMs large-scale circulation.

Therefore, in the last decades the regional climate model approach has become very popular for simulating regional climate for a limited area domain (e.g. Dickinson et al., 1989; Giorgi and Bates, 1989; Wang et al., 2004a; Barring and Laprise, 2005). It has been demonstrated that RCMs are able to improve simulations at regional scales, especially in regions with complex orography or coastlines (e.g. Giorgi, 1990; Jones et al., 1995), and are useful in understanding of the climate processes, such as cloud-radiation, and land surface processes (e.g. Pan et al., 1995; Pal and Eltahir, 2003; Wang et al., 2004b).

*Corresponding author.
e-mail: raluca.radu@meteo.inmh.ro
DOI: 10.1111/j.1600-0870.2008.00341.x

As the approach of using limited area climate models is relatively new compared to global models, validation efforts are needed in order to establish the limitations and strengths of the regional climate methodology (see Barring and Laprise, 2005). Some of the drawbacks of limited area model used as climate model have been largely discussed by many authors (e.g. Staniforth, 1997; Laprise, 2003).

RCMs have to deal with the problem of the lateral boundary conditions. Most RCMs are one-way nested into GCMs, which means there is no feedback from the local to the global dynamics. Technically this is performed by imposing the GCM coupling fields at the lateral boundaries of the limited area domain, which leads to an ill-posed problem for the partial differential equations of the RCM: the lateral condition imposed to the model variables is not an exact solution to the model equations. Warner et al. (1997) presented the potential difficulties associated with this procedure. This technique requires interpolating coarse atmospheric fields from the GCM on the limited area grid to provide time dependent lateral boundary conditions required by the limited area model at the edges of the domain. This could possibly lead to erroneous data propagating into the regional model (see Miguez-Macho et al., 2004). The Davies (1976) approach used in most RCMs to specify their lateral boundaries over a given sponge zone has been designed to ensure a better consistency between large-scale circulations of both models near the lateral boundaries. The problems associated with the use of it are presented also by McDonald (1999) underlining that lateral boundary conditions externally supplied are a potential source of errors. The same scheme can cause mass gain or loss (see Marbaix et al., 2003) because of the differences between the

total mass in RCM and the model providing large-scale data. The combination of two sets of balanced fields can result in a non-balanced field (Staniforth, 1997).

To cure this potential drawback, it has been proposed to relax large-scales inside the regional model towards available global large-scales, in order to improve consistency between GCM and RCM. The so-called spectral nudging method has been developed by Waldron et al. (1996), Kida et al. (1991) and later by von Storch et al. (2000) and Biner et al. (2000). This method was successfully applied as a complement to the traditional lateral driving of nested models and it deserves to be further investigated.

In order to validate the regional climate models several studies used idealized experiments, among which the so-called 'Big Brother Experiment' approach developed by Denis et al. (2002b) (see also de Elía et al., 2002; Denis et al., 2003; Antic et al., 2004; Dimitrijevic and Laprise, 2005; Herceg et al., 2006). In this approach, the reference climate simulation is performed using a RCM over a large domain (Big Brother). This simulation is used to drive a RCM at the same resolution after filtering out the small-scales of the Big Brother, but over a smaller domain (Little Brother) included in the large domain. Big Brother and Little Brother are then compared in terms of large-scales and small-scales at the same resolution. In these experiments the only difference between the two 'brothers' is the nesting treatment.

However, we do not define LBC needed to drive RCM by retaining only large-scales and filtering out small-scales in order to mimic the low spatial resolution of GCM, as in Big Brother experiment, but we try to reproduce the same climate in a type of perfect model assumption by comparing a RCM simulation with a GCM simulation using the same conditions (the same high-spatial resolution, the same gridpoint dynamics, the same physical parametrizations, the same surface forcing), but different geometries and the specification of lateral boundary conditions for the limited area model.

The advantage of this idealized experiment and Big Brother is that it allows no compensation of error, being able to isolate the errors resulting from the nesting technique, independently of the errors due to model defects.

In this study, we try to tackle two main issues among the RCM validation problems: first we would like to demonstrate that the RCM is able to reproduce the large-scales of the driving global model and second, we would like to prove that the generated RCM small-scales remain in agreement with the GCM small-scales. Technically, this can be achieved by comparing the RCM and GCM fields at the same spatial resolution after filtering either the small scales or the large-scales.

The paper is organized as follows: in Section 2 a short description of the used models is presented, in Section 3 the spectral nudging method is described, in Section 4 the experimental design is shown. In Section 5 the results are analysed and Section 6 represents conclusions and perspectives.

2. Model description

The global model used, Action de Recherche Petite Echelle Grande Echelle/ Integrated Forecasting System (ARPEGE/IFS), is a spectral model developed for operational numerical weather forecast by Météo-France in collaboration with European Centre for Medium-range Weather Forecast (ECMWF). Its climate version has been developed in the 90s (see Déqué et al., 1994). ARPEGE climate version has been used as the atmosphere part of the Météo-France earth modelling system (atmosphere, ocean, land-surface and sea-ice) for IPCC (2007). The full system is described by Salas y Mélia et al. (2005).

The regional model used, Aire Limitée Adaptation dynamique Développement InterNational (ALADIN), is a spectral limited area model developed for short-range regional forecast in several European countries (Bubnova et al., 1993). In this study, the ALADIN climate version used is based on cycle 24 of ARPEGE/IFS. Indeed ALADIN is a code extension inside ARPEGE/IFS software.

ARPEGE and ALADIN share the same semi-implicit semi-Lagrangian dynamics, also used in the forecast versions. As far as the physical parametrizations are concerned, ARPEGE and ALADIN climate versions use different parametrization schemes from their short-range operational counterparts. Their common set of parametrizations is briefly described below. The convection scheme is a mass–flux scheme with convergence of humidity closure developed by Bougeault (1985), the cloud scheme used is the Ricard and Royer (1993) statistical scheme and the large-scale precipitation is described by Smith (1990). The radiative scheme is derived from Morcrette (1990) and from IFS model of the ECMWF. It includes greenhouse gases (CO_2, CH_4, N_2O and CFC) in addition to water vapour and ozone. The scheme also takes into account five classes of aerosols. More details on the model's physical parametrizations can be found at http://www.cnrm.meteo.fr/gmgec/site_engl/index_en.html. ARPEGE and ALADIN both use the spectral technique (see Orszag, 1970) which means that horizontal diffusion, semi-implicit corrections and horizontal derivatives are computed with a finite family of analytical functions. For ARPEGE, these functions are the widespread spherical harmonics (Legendre functions). In the case of ALADIN, a 2-D bi-Fourier decomposition is used (see Machenhauer et al., 1987; Haugen and Machenhauer, 1993). Contrary to the globe, the domain is not periodic, so a bi-periodicization is achieved in gridpoint space by adding a so-called extension zone (see Bubnova et al., 1993) used only for Fourier transforms. The non-linear contributions to the equations are performed in gridpoint space (Radnoti and co-authors, 1995).

The version of ARPEGE used here has a spectral truncation to wavenumber 359, which corresponds to a gridpoint resolution of about 50 km. There are 31 vertical levels, mostly located in the troposphere. The time step is 15 min.

In ALADIN model the gridpoint fields can be written as:

$$Q(x, y) = \sum_{m=-M}^{M} \sum_{n=-N}^{N} Q_m^n \mathrm{e}^{im\left(\frac{2\pi}{L_x}\right)x} \mathrm{e}^{in\left(\frac{2\pi}{L_y}\right)y}, \quad (1)$$

where Q is the field, $M(2\pi/L_x)$ is the largest wavenumber considered along x-direction and $N(2\pi/L_y)$ is the largest wavenumber considered along y-direction. At each model time step, the spectral coefficients are calculated by:

$$Q_m^n = \frac{1}{(2M+1)(2N+1)} \sum_{j=0}^{2M} \sum_{k=0}^{2N} Q(x_j, y_k)\, \mathrm{e}^{-im\left(\frac{2\pi}{L_x}\right)x_j} \mathrm{e}^{-in\left(\frac{2\pi}{L_y}\right)y_k}, \quad (2)$$

where we used a regular rectangular grid with x_j and y_k as coordinates. In bi-Fourier space, each wave is represented by a couple of zonal and meridional wavenumbers (m, n) and the total effective wavenumber k is obtained here by the relationship:

$$k = \sqrt{m^2 + n^2}. \quad (3)$$

In this version, the domain covers Europe with a 50 km resolution. Its size is $L_x = 6000$ km by $L_y = 6400$ km. The spectral decomposition uses $M = 59$ and $N = 63$. There are thus 120 gridpoints along x-direction and 128 points along y-direction. ALADIN is traditionally driven by ARPEGE through the Davies technique with gridpoint relaxation of wind, temperature, moisture and surface pressure in the 8 lateral rows of ALADIN grid. The above mentioned biperiodicization zone (11 rows) is beyond this relaxation zone. It is arbitrarily set on the East and North side of the grid. The vertical discretization is the same as ARPEGE (31 levels). The time step is taken as 15 min, as for ARPEGE, although ALADIN remains stable with 30 min.

3. The spectral nudging method

It is desirable that RCM simulation develops small-scale features, dynamically consistent with the large-scales provided at its lateral boundaries and with the small-scale forcings at its lower boundary. It is known that RCM develop rapidly during a few days small-scale details, despite the fact that it is both initialized and nested by coarse-resolution data (e.g. Miyakoda and Rosati, 1977; Anthes, 1983). The small-scale features may result from small-scale surface forcings as land surface inhomogeneities and orography, but also from hydrodynamic instabilities or from non-linear interactions that lead to development of fine scale structures even in the absence of surface forcings. A global simulation with 300 km resolution is assumed to reliably describe the dynamics of the large-scales, while the RCM should be better for wave lengths less than 600 km (Laprise, 2003).

The role of spectral nudging is to relax the large-scales of the inner regional coupled model towards the large-scales supplied by the outer model. It supplies the possibly missing large-scale information and allows a smooth transition across the domain. The technique attempts to keep the simulated state close to the driving state at larger scales, while allowing the model to freely generate medium-scale features consistent with the large-scale state.

The spectral nudging scheme used in this study is similar to the spectral nudging method, originally described by Waldron et al. (1996) and later by von Storch et al. (2000), Biner et al. (2000), Miguez-Macho et al. (2004), Castro et al. (2005). Spectral nudging method can also be seen as an upscale diffusion, in which the lower part of the spatial spectrum is driven, so that the regional model better takes into account the unresolved large-scales. Symmetrically, the higher part of the GCM spectrum undergoes a traditional diffusion (squared Laplacian in ARPEGE) to better represent the unresolved small scales. Note that ALADIN uses also a classical horizontal diffusion in its smaller scales.

The method was similarly approached by Kida et al. (1991), Sasaki et al. (1995) and McGregor et al. (1998) by forcing the area averages upon the interior solution, or by insertion of large-scale state (e.g. Juang and Kanamitsu, 1994, 1997; Cocke and LaRow, 2000). The method is seen also as a 'poor person's data assimilation technique' when the regional model being forced with the large-scale weather analyses (von Storch et al., 2000).

The implementation is achieved by adding nudging terms to some prognostic dynamic fields (velocity, temperature, humidity and surface pressure) in the spectral domain with a maximum response for the large-scales and no effect for the small scales. The method is designed in order to minimize the strength of the forcing while keeping the large-scale circulation of the nested model consistent with the driving data. The relaxation is active only in the upper part of the atmosphere, so that the atmospheric variables at lower levels are let free to adjust to the surface geographical constraints (orography and physiography). A vertical variation of the nudging coefficients for each variable generally allows a smooth transition.

The fact that spectral nudging is working in spectral space makes it simple to implement in a spectral model which uses Fourier expansions in both horizontal directions like ALADIN. The method is based on the spectral representation of the ALADIN fields (Radnoti, 2001) and has been already tested in a weather forecast framework (see Radu, 2003). In ALADIN model the implementation of the spectral nudging method was done additionally to lateral relaxation method proposed by Davies.

The general spectral nudging equation for a variable is written as:

$$\frac{\partial Q}{\partial t} = \alpha(Q_{\mathrm{LS}} - Q), \quad (4)$$

where Q_{LS} is the supplied large-scale variable, Q is the limited area variable and α is the relaxation coefficient which may depend on altitude, wavenumber and atmospheric variable. After time discretization, one gets:

$$Q_{t+1} = \frac{1}{1 + \alpha\Delta t} Q_t + \frac{\alpha\Delta t}{1 + \alpha\Delta t} Q_{\mathrm{LS}}, \quad (5)$$

where Q_t and Q_{t+1} are the model variables at time steps t and $t + 1$. Δt is the time step. This form is identical to the Davies relaxation except that the coefficients of Q_t and Q_{LS} depend on space instead of wavenumber.

4. Description of the experiment

Three experimental steps were performed in this study: the first step is represented by the experiment with the global model over 25 yr which constitutes the reference against RCM simulations and also will provide the lateral boundary conditions for RCM. The second step consists in two regional climate experiments over the same period from which one employs spectral nudging, and the other not. The third step consists of two additional RCM simulations with a shorter length (12 yr) in order to test the sensitivity of the spectral nudging method.

In this study, an experimental framework of a perfect model was used in which the limited area model is driven by data generated by the same model but on a larger domain, at the same high-spatial resolution in order to prove that RCM is able to reproduce the large-scale circulation of GCM. This global model is ARPEGE. It is used as both a driving model and a reference for validation. It has been integrated over a 25-yr period 1979–2003, forced by monthly observed Sea Surface Temperature (SST) from ECMWF analyses. As stated in Section 2, it uses a global grid resolution of 50 km.

ALADIN model was integrated using a Lambert geometry grid over Europe, the same grid as used in the ENSEMBLES project (see Hewitt and Griggs, 2004). Figure 1 shows the whole domain including the Davies relaxation zone (a 400 km rim outside the thin rectangle), and an inner domain which will be used for analysis in Section 5 (inside thick rectangle). On the same figure, the mean sea level pressure systematic error of ARPEGE in DJF is shown. The aim of this paper is not a validation of the high resolution GCM. But it is important to notice that what we consider here as 'perfection' is not very far from reality. In the other seasons (not shown), the systematic error is smaller.

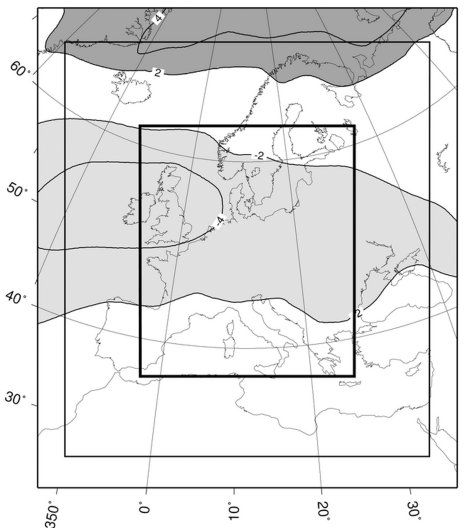

Fig. 1. Difference in mean sea level pressure between ARPEGE and ERA40 reanalysis in DJF, restricted to the ALADIN full integration domain. Contour interval 2 hPa, 0-contour not plotted, light shading below −2 hPa and dark shading above 2 hPa. The thick rectangle represents the analysis domain. The thin rectangle corresponds to the limit of the ALADIN free integration domain.

ALADIN used lateral boundary conditions from the ARPEGE integration which were provided at each 6 h, using the same surface forcing data for SST and soil/vegetation characteristics. As the spatial resolutions of ALADIN and ARPEGE are comparable (but not identical since the grid mappings are different), and as they use the same physical parametrizations, the same gridpoint dynamics, the same surface forcing, differences in the results can appear only because of the treatment of dynamics on different geometries (bi-Fourier versus Legendre filtering) or because of the specification of the lateral boundary conditions in ALADIN whereas ARPEGE is free.

The first two regional climate experiments have been carried out with ALADIN model over 25 yr (1979–2003). One experiment was performed without using spectral nudging (RCM-NN), and the other one using the technique of large-scale nudging to attempt to better nest RCM into GCM (RCM-SN1). The function used for nudging is a simple function varying with the height: 0 from surface to 880 hPa (approximately the boundary layer top), linearly increasing as a function of pressure between 880 and 750 hPa, constant above. Spectral nudging is not applied to scales smaller than 300 km (wavenumber greater than 20) and fully applied to scales larger than 400 km (wavenumber less than 15), with a linear transition in the medium spectrum. Different e-folding times were considered for a smooth relaxation. Vorticity is strongly driven (2.5 h). Temperature and surface pressure are less constrained (12.5 h), and divergence is even less (25 h). Humidity is let free in ALADIN to avoid a permanent spin-up in the physics. With such coefficients, preliminary studies using ARPEGE relaxed toward itself (twin nudging) show that the driven integration is identical to the driving one.

In addition, two sensitivity experiments were performed with ALADIN model using large-scale nudging over 12 yr covering 1979–1990 period. In the first one, named RCM-SN2, temperature is not nudged and the rest is kept the same as the experiment configuration of RCM-SN1. In the other one (RCM-SN3), specific humidity is nudged with the same e-folding time as temperature and surface pressure (12.5 h), the other variables being processed as in RCM-SN1.

5. Results

We study here to what extent spectral nudging is able to avoid the deviation of RCM from the large-scale part of the GCM, considered here as the perfection to be reached. By introducing

non-physical terms into the equations, it may be expected, due to non-linearity, that the small-scale part of the RCM will be affected, and thus diverges from the small scale part of the GCM. On the other hand, using a better large-scale may improve the small scale, versus the non-nudged RCM. In order to minimize the fact that small-scale information is injected at the lateral boundaries of the RCM, we will discard a 1000 km strip on four sides of the free domain to restrict our diagnostic area (see Fig. 1).

5.1. Mean temperature and precipitation

Among several aspects of model results that should be evaluated, the most frequently studied is the time mean climate defined by multidecadal seasonal means of meteorological variables, as near-surface temperature, precipitation and sea level pressure which are of major interest.

The fields of 2 m temperature and precipitation have been chosen here for the analysis because they are strongly influenced by the large-scale flow patterns (as advection or cyclonic activity), but exhibit small-scale features. They are not directly large-scale nudged because spectral nudging is applied above 750 hPa for temperature in the simulation RCM-SN1, but when nudging specific humidity (RCM-SN3) it is noticed the influence in a big extent in the resulted precipitation. Figure 2 shows the differences in 2 m temperature between the driving GCM and the RCM not nudged (RCM-NN) and RCM spectrally nudged (RCM-SN).

The analysis of RCM-NN and RCM-SN1 results obtained for the first 12 yr interval (noted with RCM-NNa and RCM-SN1a) are consistent with the analysis performed for the last 12 yr (RCM-NNb and RCM-SN1b), which indicates that our results are statistically significant for a shorter length period.

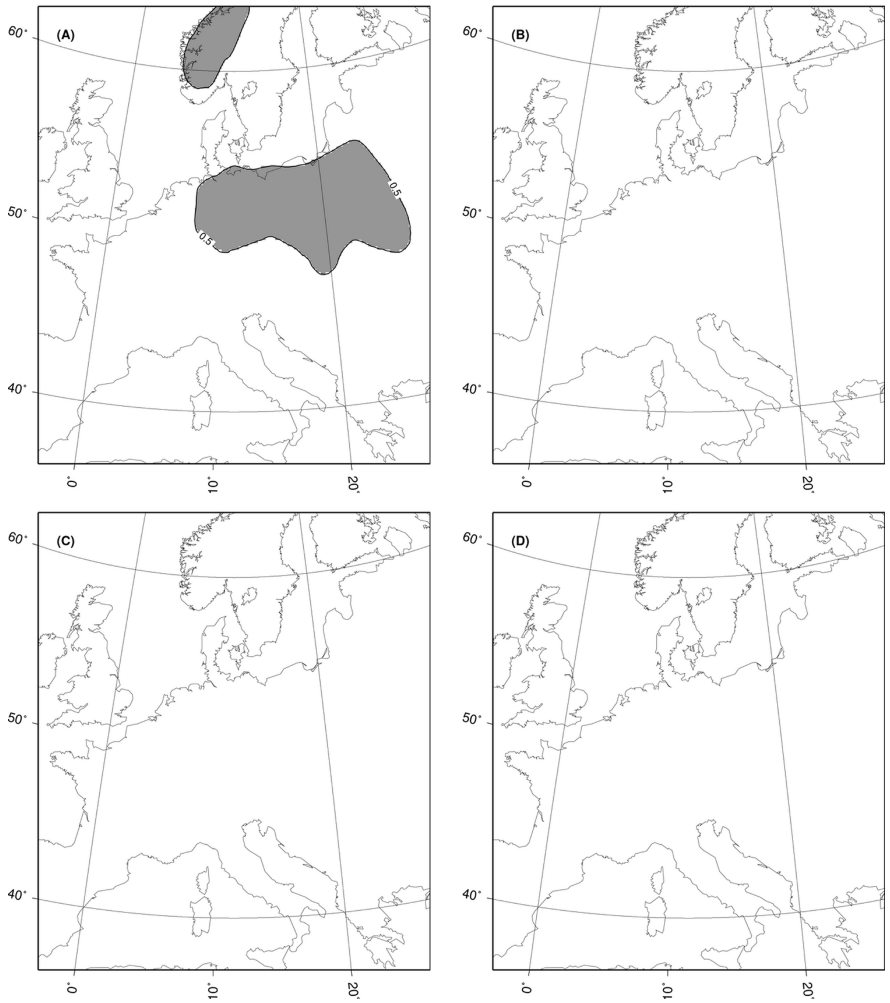

Fig. 2. Differences in 2m temperature between ARPEGE and ALADIN without spectral nudging (RCM-NN) and with spectral nudging (RCM-SN) in winter (DJF): RCM-NNa [top left-hand side, (A)]; RCM-SN1a [top right-hand side, (B)]; RCM-SN2a [bottom left-hand side, (C)] and RCM-SN3a [bottom right-hand side, (D)]. Contour interval 0.5 K, 0-contour omitted, light shading below −0.5 K and dark shading above 0.5 K.

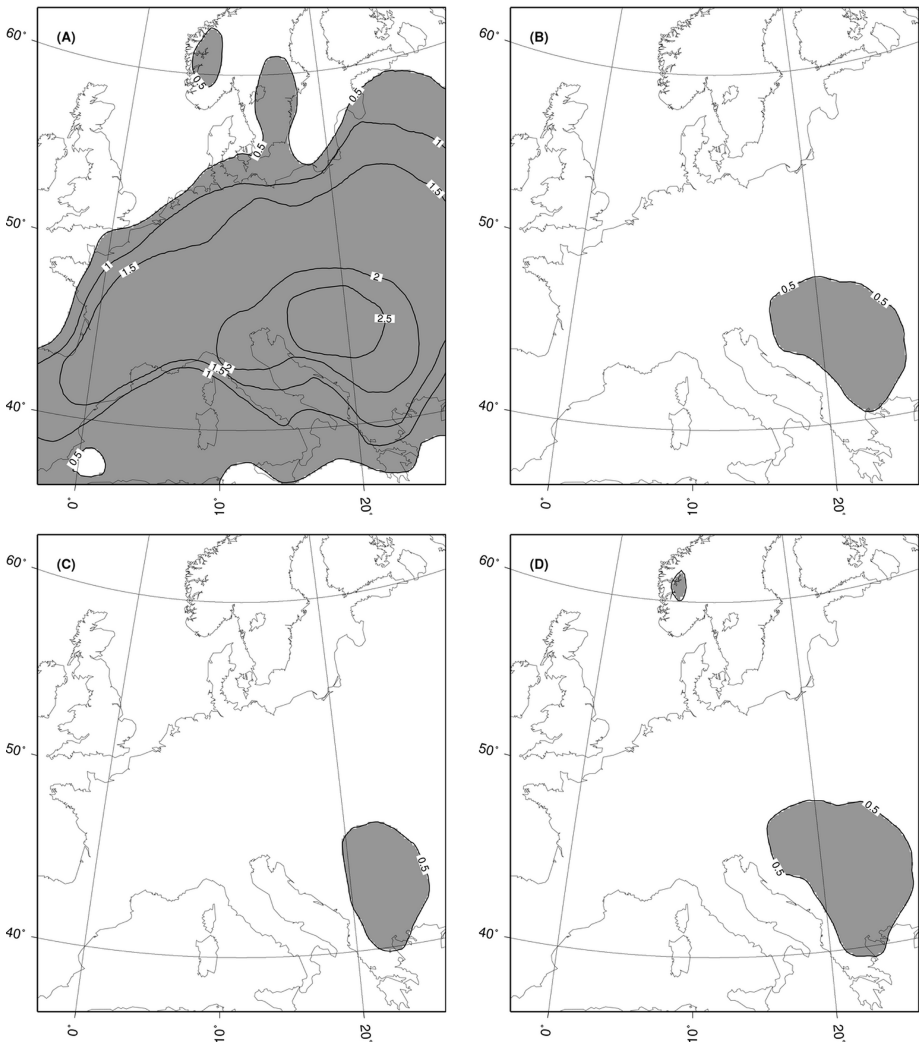

Fig. 3. As Fig. 2, but for 2m temperature in summer (JJA) RCM-NNa [top left-hand side, (A)]; RCM-SN1a [top right-hand side, (B)]; RCM-SN2a [bottom left-hand side, (C)] and RCM-SN3a [bottom right-hand side, (D)]. Contour interval 0.5 K, 0-contour omitted, light shading below −0.5 K and dark shading above 0.5 K.

Seasonal means have been computed over 12 yr (1979–1990) for winter (DJF) and summer (JJA). In both seasons RCM-SN1a is very close to the GCM. In winter, RCM-NNa agrees with GCM, except a small positive bias over North Europe. In summer, Fig. 3 [top left-hand side, (A)], an overall warm bias is observed over continent in RCM-NNa (the same SST being prescribed, the difference is weak over sea). This bias reaches 2.5 K over Southeast Europe. This problem of warming of Southeast Europe in regional simulations over last years was largely debated in many papers related to PRUDENCE project (`http://prudence.dmi.dk/`). When the large-scales are nudged (RCM-SN1), Fig. 3 shows that spectral nudging succeeds in removing this bias, which is due to the large-scale nudging of velocity and surface pressure [Fig. 3 bottom left-hand side, (C)] and not of temperature and humidity in the upper atmosphere.

For precipitation, things are somewhat less simple. In winter, Fig. 4 [top right-hand side, (B)], a 0.5 mm d^{-1} wet bias appears in RCM-SN1 over the North Sea. In summer, Fig. 5 [top left-hand side, (A)] a 0.5 mm d^{-1} dry bias affects most continental part in RCM-NN. The latter shortcoming is worse than the former, because of the size of the area concerned in summer, and because the wet bias in winter occurs in a very rainy area. There are thus a big error, in summer, which can be easily related to the 2 m temperature bias through a well known positive feedback in hot and dry summers (Rowell and Jones, 2006), and a smaller one, in winter, which appears to be a side effect of the spectral nudging.

With the aim of exploring the relative role of the nudged variables by assessment of the uncertainties effect, two sensitivity tests by using different nudged variables have been realized. The sensitivity of RCM to the dynamics of all the upper nudged variables is noticed when analysing the pattern of precipitation

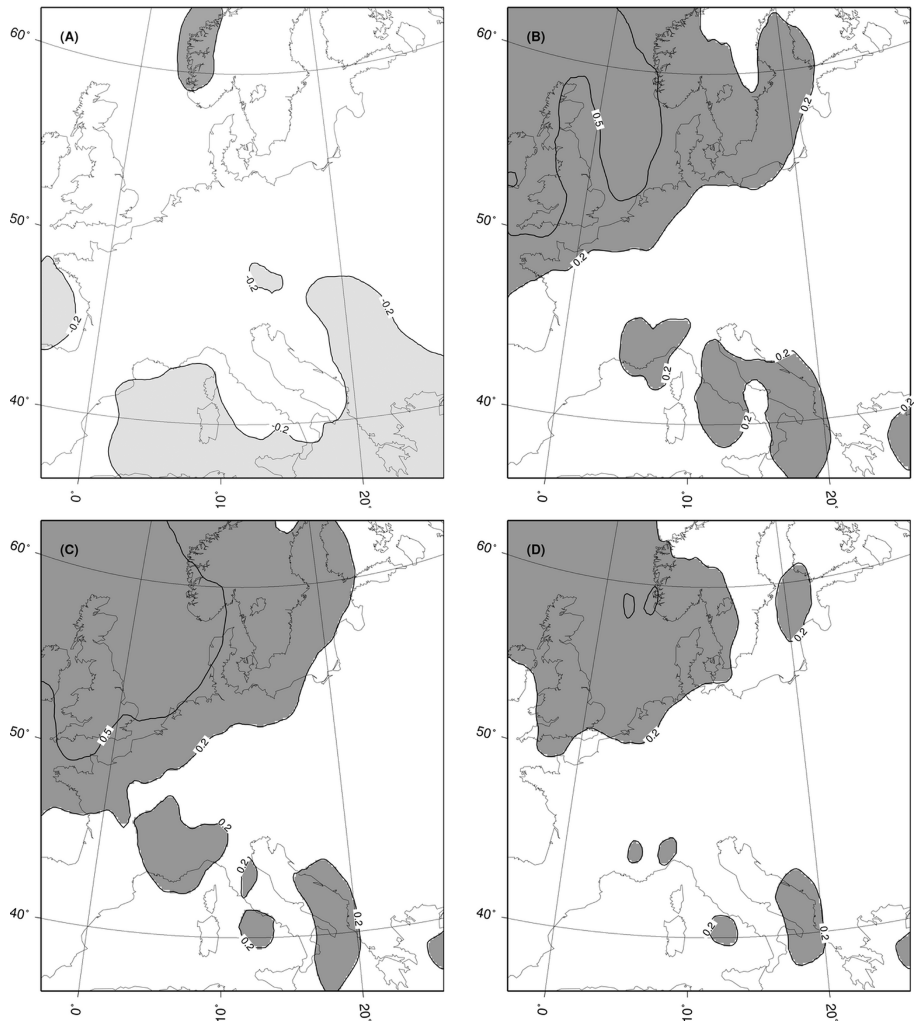

Fig. 4. As Fig. 2, but for precipitation in winter (DJF) RCM-NNa [top left-hand side, (A)]; RCM-SN1a [top right-hand side, (B)]; RCM-SN2a [bottom left-hand side, (C)] and RCM-SN3a [bottom right-hand side, (D)]. Contours ± 0.2 mm d^{-1}, ± 0.5 mm d^{-1}, ± 1 mm d^{-1}, light shading below -0.2 mm d^{-1} and dark shading above 0.2 mm d^{-1}.

in the RCM-SN3 simulation. By nudging specific humidity towards the values of the large-scale driving data, the artificially increased precipitation in winter was significantly reduced to 0.25 mm d^{-1} over the Northeastern part of the domain [Fig. 4 bottom right-hand side, (D)] and the dry bias from summer over the continental area was removed.

From these results, we can conclude that for 2m temperature spectral nudging is able to improve RCM by removing the difference between GCM and RCM both in winter and summer. For precipitation the results using spectral nudging are also better both in summer and in winter, but those can be achieved just by performing sensitivity tests in order to choose the suitable configuration for proper nudging of variables. One should be aware of the fact that the specific humidity plays an important role.

Warmer temperatures in summer in RCM-NN goes to quicker soil dryness, which means decreased evaporation, as consequence reduced precipitation over Europe. Improved RCM results with RCM-SN1a can be attributed to the fact that advection is nudged whereas humidity is not, the model being free to develop its own moisture dynamics. By nudging specific humidity the model is able to correct the precipitation pattern, which underlines the RCM strategy of using the same physics as its driving model to achieve a maximum compatibility between the nested and driving models.

5.2. *Scale decomposition*

At this stage, it is important to compute error budgets separately for the large-scale and for the small-scale. A spatial and temporal scales decomposition method has been used in spectral nudging analysis by Denis et al. (2002a) and by Feser and von Storch (2006). A simple spectral filter is built similarly to eqs (1) and (2). This filter is able to separate the fields of the models

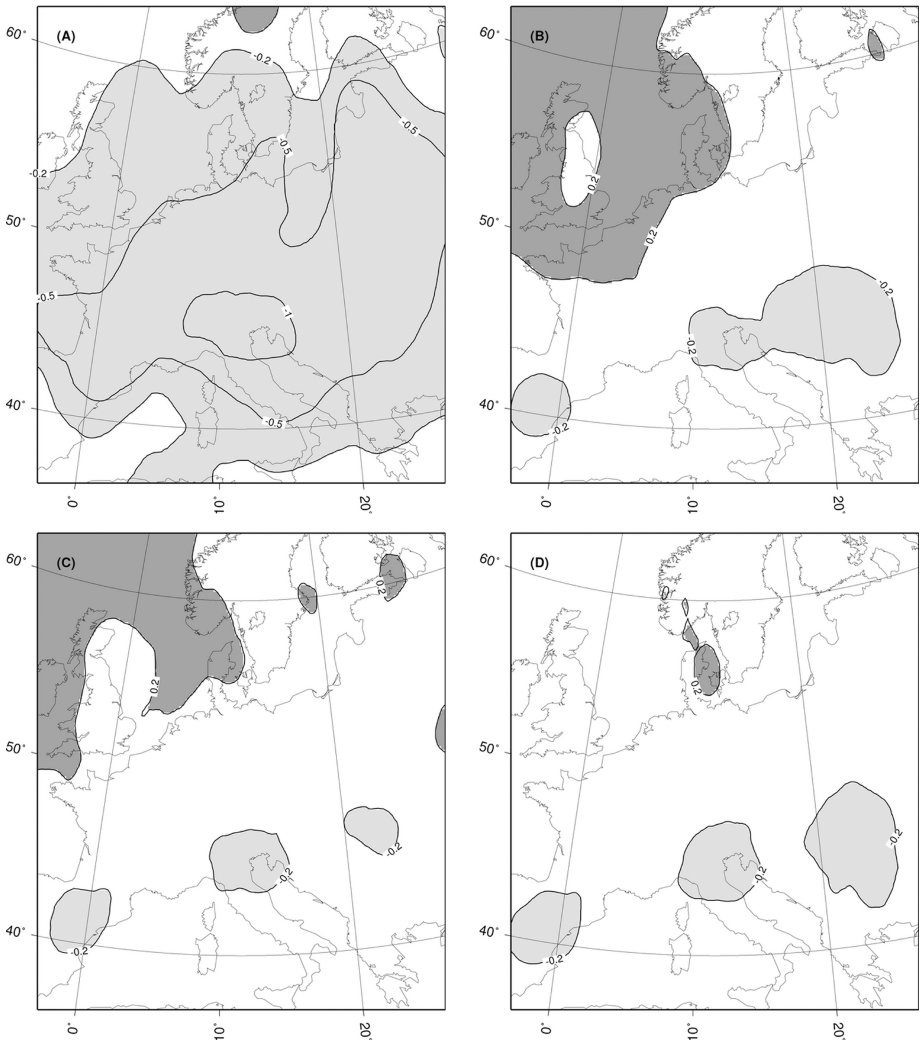

Fig. 5. As Fig. 2, but for precipitation in summer (JJA) RCM-NNa [top left-hand side, (A)]; RCM-SN1a [top right-hand side, (B)]; RCM-SN2a [bottom left-hand side, (C)]; RCM-SN3a [bottom right-hand side, (D)]. Contours ± 0.2 mm d^{-1}, ± 0.5 mm d^{-1}, ± 1 mm d^{-1}, light shading below -0.2 mm d^{-1} and dark shading above 0.2 mm d^{-1}.

into different spatial scales by removing some wavenumbers (m, n). The bi-dimensional filter was applied to the inner domain (Fig. 1, thick rectangle). The filter was applied to separate large-scale components of above 600 km (typical of the GCM) and small-scale components below 300 km (the part of the spectrum which is not relaxed in ALADIN).

In order to complete the assessment of the RCM against the 'perfect' GCM, the large-scale and small-scale components of the fields were split into transient and stationary parts. Each field was decomposed into its time mean (overbarred) and time deviation (prime):

$$Q(x,t) = \overline{Q(x)} + Q'(x,t). \tag{6}$$

The time averaging was performed for each calendar month separately, so that errors in the mean annual cycle are accounted for in the stationary part, not in the transient one. This method was applied to daily values of 2m temperature and precipitation and to 6-hourly values of mean sea level pressure (MSLP). The root mean square differences (RMSD) are presented in Table 1, 3, 5 for winter and in Table 2, 4, 6 for summer.

In winter, the tables show that for all variables the large scales are, as expected, better with spectral nudging than without. MSLP is the only field directly nudged (in fact relaxation is applied to surface pressure). The sea level pressure field is interesting as it provides a vertically integrated measure of the mass distribution in the atmosphere, but it has to be interpreted with caution in the high topography regions. The MSLP day-to-day correlations of RCM-NN and RCM-SN1 with the driver as function of wavenumber are very high for low-spectrum (not shown). In addition, the stationary small-scale component of the MSLP field demonstrates no influence in small-scales induced by large-scales modification in the simulations with spectral nudging of

Table 1. Root mean square difference (RMSD) of regional climate model without (RCM-NN) and with (RCM-SN) spectral nudging versus the driving global model (GCM); stationary and transient large-scale and small scale components for daily temperature (K) in winter (DJF)

EXP	Stat. LS	Stat. SS	Tran. LS	Tran. SS
RCM-NN a	1.19	0.76	1.69	0.60
RCM-SN1 a	1.17	0.78	1.13	0.57
RCM-SN2 a	1.17	0.78	1.13	0.58
RCM-SN3 a	1.16	0.77	1.12	0.58
RCM-NN b	1.05	0.76	1.76	0.63
RCM-SN b	1.09	0.77	1.09	0.59

Table 2. As Table 1 for daily temperature (K) in summer (JJA)

EXP	Stat. LS	Stat. SS	Tran. LS	Tran. SS
RCM-NN a	1.27	0.55	2.01	0.64
RCM-SN1 a	0.50	0.50	1.07	0.58
RCM-SN2 a	0.46	0.49	1.11	0.58
RCM-SN3 a	0.54	0.50	1.11	0.58
RCM-NN b	1.60	0.54	2.47	0.65
RCM-SN1 b	1.05	0.49	1.95	0.59

Table 3. As Table 1 for precipitation (mm d^{-1}) in winter (DJF)

EXP	Stat. LS	Stat. SS	Tran. LS	Tran. SS
RCM-NN a	0.48	0.34	2.79	1.25
RCM-SN1 a	0.57	0.35	2.38	1.20
RCM-SN2 a	0.60	0.36	2.56	1.24
RCM-SN3 a	0.52	0.36	2.39	1.21
RCM-NN b	0.69	0.38	3.33	1.42
RCM-SN1 b	0.78	0.41	2.69	1.35

temperature and specific humidity. The MSLP of RCM which is generally controlled by large-scale circulation, is recovered in its small-scale components at the same level of skill in winter as in summer.

There is an exception for large-scales stationary precipitation which is slightly degraded with spectral nudging, when specific humidity is not nudged (RCM-SN1). This is a confirmation of the results in Fig. 4. The large-scale precipitation improvement is obtained by specific humidity nudging [shown in Fig. 4 bottom right-hand side, (D) and in Table 3]. As far as the small scales are concerned, the RCMs have closer scores in the stationary part (i.e. the bias is the same in quadratic average) and with small difference in the transient part.

In summer (Tables 2 and 4) the results are even more spectacular for the large-scales because the improvement is clear also for the stationary part (as expected from Section 5.1). For the small scales (stationary and transient), there is very small improvement with spectral nudging for 2m temperature. We obtain a better result in both large and small-scales components for precipitation when nudging large-scales of specific humidity.

Table 4. As Table 1 for precipitation (mm d^{-1}) in summer (JJA)

EXP	Stat. LS	Stat. SS	Tran. LS	Tran. SS
RCM-NN a	0.56	0.30	3.61	1.53
RCM-SN1 a	0.35	0.31	2.31	1.46
RCM-SN2 a	0.34	0.30	2.55	1.50
RCM-SN3 a	0.31	0.31	2.36	1.48
RCM-NN b	0.50	0.32	3.56	1.54
RCM-SN1 b	0.38	0.32	2.35	1.49

Table 5. As Table 1 for mean sea level pressure (hPa) in winter (DJF)

EXP	Stat. LS	Stat. SS	Tran. LS	Tran. SS
RCM-NN a	0.70	0.06	2.88	0.08
RCM-SN1 a	0.46	0.06	2.23	0.08
RCM-SN2 a	0.45	0.06	2.22	0.08
RCM-SN3 a	0.42	0.06	2.12	0.08
RCM-NN b	0.74	0.06	3.09	0.08
RCM-SN1 b	0.41	0.06	2.05	0.08

Table 6. As Table 1 for mean sea level pressure (hPa) in summer (JJA)

EXP	Stat. LS	Stat. SS	Tran. LS	Tran. SS
RCM-NN a	0.57	0.07	2.75	0.08
RCM-SN1 a	0.28	0.06	1.09	0.07
RCM-SN2 a	0.21	0.06	1.15	0.07
RCM-SN3 a	0.25	0.06	1.11	0.07
RCM-NN b	0.59	0.06	2.58	0.08
RCM-SN1 b	0.28	0.06	1.04	0.07

The stationary RMSD is just a measure of what we can see in Figs. 2–5. The transient RMSD indicates how correlated the day-to-day variations of the RCM are with respect to the GCM. It can be compared to the standard deviation of the GCM: as long as RMSD is less than $\sqrt{2}$ times the standard deviation, the time evolution of the RCM and GCM are positively correlated. Our results show that this is true for the large scales. In winter, $\sqrt{2}$ times the standard deviation is 4.4 K, 15.7 hPa and 5.4 mm d^{-1} for the three fields of Table 1, 3 and 5. In summer, we get 3.1 K, 7.3 hPa and 4.6 mm d^{-1}, respectively. However, when such scores are calculated for the small scales, we obtain the same values as in the tables. This indicates that the small scales generated by the RCMs are independent of the GCM. Thus, the fact that the spectral nudging does not degrade the transient small scales indicates simply that the two RCM 'noises' have the same statistical properties. We cannot state that RCMs' small scales follow those of the GCM. We have also calculated the RMSD between RCM-NN and RCM-SN. The transient part of the small

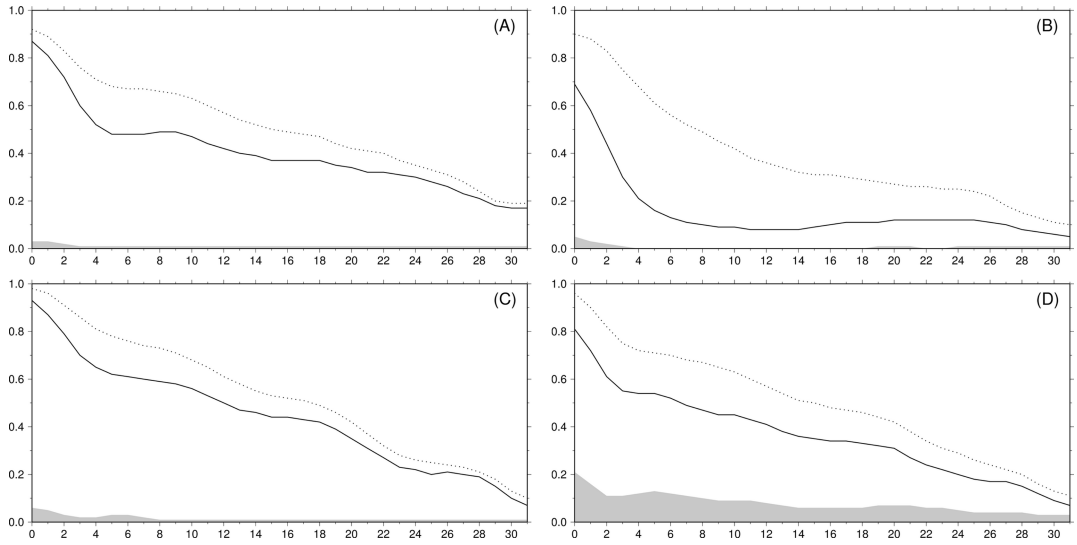

Fig. 6. RCM-NN day-to-day correlation with GCM (full line) compared with RCM-SN (dotted-line) as a function of spatial wavenumber: Precipitation in winter [top left-hand side, (A) and in summer [top right-hand side, (B)]; 2m temperature in winter [bottom left-hand side, (C)] and in summer [bottom right-hand side, (D)]. The grey area represents 95% interval of independent experiments.

scales exhibits the same values: the two RCMs are independent of each other.

The analysis of correlation spectra allows to compare the contribution of different scales to RCM-NN and RCM-SN1 against GCM solutions in Fig. 6. In this way, the arbitrary cut-off wavenumber can be avoided and this indicates below which scales RCM becomes independent of GCM. The grey area represents 95% interval of independent experiments, which was calculated by scrambling RCM series with respect to GCM chronology. It shows that for 2 m temperature and precipitation low-spectrum both RCM are better correlated with GCM in winter, than in summer. It is noticed also a weaker correlation RCM/GCM in grey area of small-scales.

If RCMs are perfectly correlated, closer to value 1, it means that the RCM and GCM are almost synchronized, predicting small variance when small and a large one when there is large one. However, when considering the direct relationship between RCM-NN and RCM-SN1 it is observed that for stationary and transient small-scales components, the models have quite similar evolution, with better correlation for RCM-SN1 for 2m temperature and precipitation (Fig. 6). This conclusion is sustained also by the RMSD values from the presented tables. As for low-wave numbers (large-scales) we notice different behaviour, where quite big differences between RCM-NN and RCM-SN1 are in summer.

5.3. Precipitation extremes

Regional models are used to spatially refine the mean climatology of a given field, but also to tell something about extreme events. Indeed extreme events are generally local, especially when they are violent (storms, floods). We address here the question whether the simulated extreme precipitation in summer and winter with the RCM spectrally nudged show similar characteristics with those simulated in the GCM. For each gridpoint of the analysis domain, the percentiles of daily precipitation in both seasons have been computed. In Fig. 7 the 90–99% precipitation quantiles averaged over the domain (see Fig. 1) are displayed. Several inferences can be drawn from this picture. It can be seen that RCM-SN1 distribution is closer to GCM distribution in summer than in winter, a fact also noticed in Fig. 4. RCM-SN1 increases artificially the extreme precipitation in winter. This increase is obtained for all percentiles (not shown), but it is larger, even in relative value, for the upper percentiles. This represents a weak amount in terms of precipitation (2 mm d^{-1} for a base value of 20 mm d^{-1}), but in terms of frequency the event 'precipitation above 15 mm d^{-1}' increases by 50%. In summer, there is underestimation of precipitation in the RCM-NN model, the large-scale nudging showing amounts closer to the GCM [see Fig. 7 (right-hand side)]. But we can suspect an error compensation between a drying due to RCM and a moistening due to spectral nudging. The spurious precipitation increase already mentioned in Section 5.1 is thus an increase in heavy precipitation events when specific humidity is not nudged. We can see with the help of the perfect model approach that GCM and RCM tend to underestimate heavy precipitation events (Frei et al., 2003). With the standard approach, we would have concluded that spectral nudging improves the regional simulation by allowing more intense precipitation events.

6. Conclusions and perspectives

In this paper the performance of a regional climate model was studied in a perfect model approach, represented here by a driver

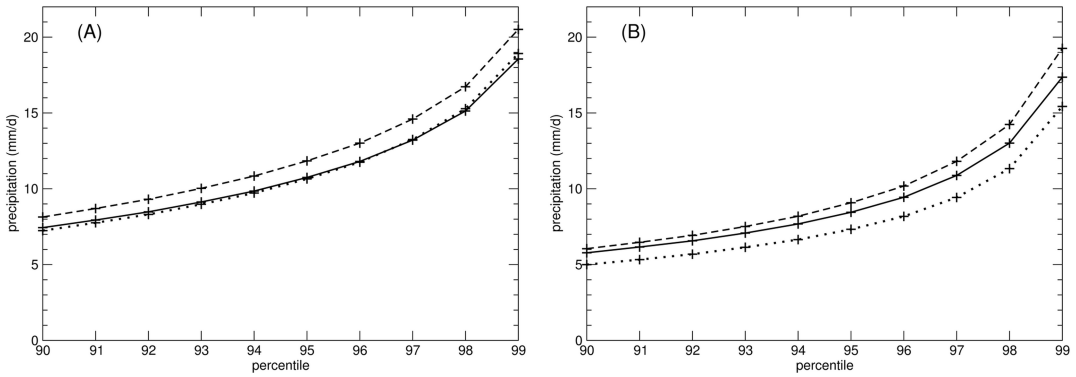

Fig. 7. Percentiles of precipitation (mm d^{-1}) averaged over the domain of analysis in winter [left-hand side, (A)] and summer [right-hand side, (B)]: GCM in solid line, RCM without spectral nudging in dotted line, RCM with spectral nudging in dashed line.

global high resolution model. Our purpose was to prove one of the main aims of the regional climate models: RCMs are able to maintain the large-scale circulation of the driving GCM, modifying only the smaller scales. The goal was also to demonstrate within the idealized experimental frame in multidecadal and decadal simulations, the potential and the feasibility of the spectral nudging method, seen as solution to overcome LBC limitations.

It has be shown that spectral nudging method is able to avoid the deviation of the RCM from the GCM in the spatial scales typical of the GCM (wave length of 600 km and above). This is true for the mean climate (stationary part) as well as for the day-to-day variability (transient part). As far as the smallest scales are concerned, we found very little predictability in the meteorological sense (so called butterfly effect). However, the statistical properties of these small scales (predictability in climatic sense) are not degraded by the effect of relaxation of the lower part of the spectrum.

In addition, it was found that spectral nudging tends to artificially increase intense precipitation events in winter when specific humidity is not relaxed. On the other hand, the summer warm bias can be corrected by relaxing only velocity and surface pressure. The proposed scheme succeeds to provide possibly missing large-scale information to the regional climate model, removing some imbalances resulting from the specification at the lateral boundary. This is particularly important when the RCM domain is large and the RCM is able to develop large-scale features in the centre of the domain which disagree with the solution imposed at the boundaries.

These results were achieved without performing any tuning of the nudging parameters, leaving room for further improvement. Indeed the choice of the configuration was dictated by low resolution GCM experiments carried out several years ago. Ongoing work is focusing on finding the optimal configuration of the spectral nudging coefficients. Another remaining question to address is the added value of the RCM. Here the RCM is nothing more than a local replay of the driving GCM. Further studies introducing spatial filtering of LBC (mimicking a low resolution GCM) are necessary to evaluate to which extent an RCM is able to recover the stationary and transient aspects of the high resolution simulation. The perfect model approach is an efficient way to perform clean sensitivity experiments, without being polluted by model error compensation. However spectral nudging experiments are planned with ERA40 and climate change scenario forcing.

7. Acknowledgments

This project was partly supported by European Commission FP-6 projects ENSEMBLES (GOCE-CT-2003-505539) and CECILIA (GOCE-CT-2006-037005). The authors would like to thank Nellie Elguindi and Jure Jerman for helpful suggestions and comments on the work or the manuscript.

References

Anthes, R. A. 1983. Regional models of the atmosphere in middle latitudes. *Mon. Wea. Rev.* **111**, 1306–1335.

Antic, S., Laprise, R., Denis, D. and de Elía, R. 2004. Testing the downscaling ability of a one-way nested regional climate modeling regions of complex topography. *Clim. Dyn* **23**, 473–493.

Barring, L. and Laprise, R. 2005. High-resolution climate modelling: Assesment, added value and applications. In: *Extendend abstracts of a WMO/WCRP-sponsored regional scale climate modelling Workshop Lund (Sweden), 29 March-2 April 2004*, Lund University electronic reports in physical geography 132 pp.

Biner, S., Caya, D., Laprise, R. and Spacek, L. 2000. Nesting of RCM by imposing large scales. *WMO/TD No. 987* **30**, 7.3–7.4.

Bougeault, P. 1985 A simple parameterization of the large-scale effects of cumulus convection. *Mon. Wea. Rev.* **113**, 2108–2121.

Bubnova, R., Horányi, A. and Malardel, S. 1993. International project ARPEGE/ALADIN. *EWGLAM Newslett.* **22**, 117–130.

Castro, C. L., Pielke, R. A. Sr. and Leoncini, G. 2005. Dynamical downscaling: an assessment of value added using regional climate model. *J. Geophys. Res.-Atmos.* **110**, D05108, doi:10.1029/2004JD004721.

Cocke, S. and LaRow, T. E. 2000. Seasonal predictions using a regional spectral model embedded within a coupled ocean-atmosphere model. *Mon. Wea. Rev.* **128**, 689–708.

Davies, H. C. 1976. A lateral boundary formulation for multi-level prediction models. *Quart. J. Roy. Meteor. Soc.* **102**, 405–418.

de Elía, R., Laprise, R. and Denis, B. 2002. Forecasting skill limits of nested, limited area models: a perfect model approach. *Mon. Wea. Rew.* **130**, 2006–2023.

Denis, B., Côté, J. and Laprise, R. 2002a. Spectral decomposition of two-dimensional atmospheric fields on limited-area domains using the discrete cosine transform (DCT). *Mon. Wea. Rew* **130**, 1812–1829.

Denis, B., Laprise, R., Caya, D. and Côté, J. 2002b. Downscaling ability of one-way nested regional climate models: the Big-Brother Experiment. *Clim. Dyn.* **18**, 627–646.

Denis, B., Laprise, R. and Caya, D. 2003. Sensitivity of a regional climate model to the spatial resolution and temporal updating frequency of the lateral boundary conditions. *Clim. Dyn.* **20**, 107–126.

Déqué, M., Dreveton, C., Braun, A. and Cariolle, D. 1994. The ARPEGE-IFS atmosphere model: a contribution to the French community climate modelling. *Clim. Dyn.* **10**, 249–266.

Dickinson, M., Errico, R. M., Giorgi, F. and Bates, G. T. 1989. A regional climate model for the western United States. *Clim. Change* **15**, 383–422.

Dimitrijevic, M. and Laprise, R. 2005. Validation of the nesting technique in a regional climate model and sensitivity tests to the resolution of the lateral boundary conditions during summer. *Clim. Dyn.* **25**, 555–580.

Feser, F. and von Storch, H. 2006. A spatial two-dimensional discrete filter for limited area model evaluation purposes. *Mon. Wea. Rev.* **133**, 1774–1786.

Fouquart, Y. 1987. Radiative transfer in climate modeling. In: *NATO Advanced Study Institute on Physically-Based Modeling and Simlation of Climate and Climatic Changes. Erice, 11–23 May 1986*. (ed. M. E. Schlesinger, 223–283).

Frei, C., Christensen, J. H., Déqué, M., Jacob, D., Jones, R. G. and Vidale, P. L. 2003. Daily precipitation statistics in regional climate models: evaluation and intercomparison for the European Alps. *J. Geophys. Res.* **108**, ACL 91–19.

Giorgi, F. 1990. Simulation of regional climate using a limited area model nested in general circulation model. *J. Climate* **3**, 941–963.

Giorgi, F. and Bates, G. T. 1989. On the climatological skill of a regional model over complex terrain. *Mon. Wea. Rev.* **117**, 2325–2347.

Herceg, D., Sobel, A. H., Sun, L. and Zebiak, S. E. 2006. The Big Brother experiment and seasonal predictability in the NCEP regional spectral model. *Clim. Dyn.* **27**, 69–82.

Haugen, J. E. and Machenhauer, B. 1993. A spectral limited-area model formulation with time dependent boundary conditions applied to the shallow-water equations. *Mon. Wea. Rev.* **121**, 2618–2630.

Hewitt, C. D. and Griggs, D. J. 2004. Ensembles-based predictions of climate changes and their impacts. *EOS* **85**, 566.

IPCC, 2007. Climate Change 2007: the Physical Science Basis. In: *Contribution of Working Group I to the Fourth Assessment Report of the Intergovernmental Panel on Climate Change* (eds S. Solomon, D. Qin, M. Manning, Z. Chen, M. Marquis and co-editors), Cambridge University Press, Cambridge, United Kingdom and New York, NY, USA.

Jones, R. G., Murphy, J. M. and Noguer, M. 1995. Simulation of climate change over Europe using a nested regional-climate model. Part I: assesment of control climate, including sensitivity to location of lateral boundaries. *Quart. J. Roy. Meteor. Soc.* **121**, 1413–1449.

Juang, H.-M. H. and Kanamitsu, M. 1994. The NMC regional spectral model. *Mon. Wea. Rev.* **122**, 3–26.

Juang, S.-Y. H. and Kanamitsu, M. 1997. The NCEP regional spectral model: an update. *Bull. Amer. Meteor. Soc.* **78**, 2125–2143.

Kida, H., Koide, T., Sasaki, H. and Chiba, M. 1991. A new approach to coupling a limited area model with a GCM for regional climate simulation. *J. Meteor. Soc. Japan* **69**, 723–728.

Laprise, R. 2003. Resolved scales and nonlinear interactions in limited-area models. *J. Atmos. Sci.* **60**, 768–779.

Machenhauer, B. and Haugen, J.-E. 1987. Test of a spectral limited area shallow water model with time dependent lateral boundary conditions and combined normal mode/semi-Lagrangean time integration schemes. In: *ECMWF Workshop Proceedings: Techniques for Horizontal Discretization in Numerical Weather Prediction Models* ECMWF 361–371.

Marbaix, P., Galle, H., Brasseur, O. and van Ypersele, J.-P. 2003. Lateral boundary conditions in regional climate models: a detailed study of the relaxation procedure. *Mon. Wea. Rev.* **131**, 461–479.

McDonald, A. 1999. A review of lateral boundary conditions for limited area forecast models. *Proc. Ind. Natl. Sci. Acad.* **65**, 91–105.

McGregor, J. L., Katzfey, J. J. and Nguyen, K. C. 1998. Fine resolution simulations of climate change for southeast Asia. *South-east Asian Regional Committee for START Research project Final Report* 51pp. Available from CISRO Atmospheric Research, PMB1, Aspendale, VIC 3195, Australia.

Miguez-Macho, G., Stenchikov, G. L. and Robock, A. 2004. Spectral nudging to eliminate the effects of domain position and geometry in regional climate model simulations. *J. Geophys. Res.* **109**, D13104, doi:10.1029/2003JD004495.

Miyakoda, K. and Rosati, A. 1977. One way nested grid: the interface conditions and the numerical accuracy. *Mon. Wea. Rev.* **105**, 1092–1107.

Morcrette, J. J. 1990. Impact of changes to the radiation transfer parameterizations plus cloud optical properties in the ECMWF model. *Mon. Wea. Rev* **118**, 847–873.

Orszag, S. A. 1970. Transform method for the calculation of vector-coupled sums: application to the spectral form of the vorticity equation. *J. Atmos. Sci.* **27**, 890–895.

Pan, Z., Segal, M., Turner, R. and Tackle, E. 1995. Model simulation of impacts of transient surface wetness on summer rainfall in the United States Midwest during drought and flood years. *Mon. Wea. Rev.* **123**, 1575–1581.

Pal, J. S. and Eltahir, E. A. B. 2003. A feedback mechanism between soil-moisture distribution and storm tracks. *Quart. J. Roy. Meteor. Soc.* **129**, 2279–2297.

Radnoti, G. and co-authors, 1995. The spectral limited area model ARPEGE/ALADIN. *PWPR Report Series* **7**, *WMO-TD* **699**, 111–117.

Radnoti, G. 2001. An improved method to incorporate lateral boundary conditions in a spectral limited area model. *ALADIN Newslett.* **20** http://www.cnrm.meteo.fr/aladin/newsletters/newsletters. html

Radu, R. 2003. Extensive study of the coupling problem for a high resolution limited area model. *ALATNET Final Report* http://www.cnrm.meteo.fr/alatnet/.

Ricard, J. L. and Royer, J. F. 1993. A statistical cloud scheme for use in AGCM. *Ann. Geophys.* **11**, 1095–1115.

Rowell, D. P. and Jones, R. 2006. Causes and uncertainty of future summer drying over Europe. *Clim. Dyn.* **27**, 281–299.

Salas y Mélia, D., Chauvin, F., Déqué, M., Douville, H., Guèrèmy, J. F. and co-authors. 2005. Description and validation of CNRM-CM3 global coupled climte model. *Note de centre GMGEC, CNRM* **103**.

Sasaki, H., Kida, J., Koide, T. and Chiba, M. 1995. The performance of a long-term integrations of a limited area model wit the spectral boundary coupling method. *J. Meteor. Soc. Japan* **73**, 165–181.

Smith, R. N. B. 1990. A scheme for predicting layer clouds and their water content in a general circulation model. *Quart. J. Roy. Meteor. Soc.* **116**, 435–460.

Staniforth, A. 1997. Regional modeling: a theoretical discussion. *Meteor. Atmos. Phys.* **63**, 15–29.

von Storch, H., Langenberg, H. and Feser, F. 2000. A spectral nudging technique for dynamical downscaling purposes. *Mon. Wea. Rev.* **128**, 3664–3673.

Waldron, K. M., Paegle, J. and Horel, J. D. 1996. Sensitivity of a spectrally filtered and nudged limited area model to outer model options. *Mon. Wea. Rev.* **124**, 529–547.

Wang, Y., Leung, L.-R., McGregor, J. L., Lee, D.-K., Wang W.-C. and co-authors. 2004a. Regional climate modelling: progress, challenges and prospects. *J. Meteor. Soc. Japan* **82**, 1599–1628.

Wang, Y., Xie, S.-P., Xu, H. and Wang, B. 2004b. Regional model simulations of boundary layer clouds over the Sotheast Pacific of South America. Part I: control experiment. *Mon. Wea. Rev.* **132**, 274–296.

Warner, T. T., Peterson, R. A. and Treadon, R. E. 1997. A tutorial on lateral conditions as a basical and potentially serious limitation to regional numerical weather prediction. *Bull. Amer. Meteor. Soc.* **78**, 2599–2617.